

## Supporting Information

### Fabrication of Conjugated Microporous Polytriazine Nanotubes and Nanospheres for Highly Selective CO<sub>2</sub> capture

#### Section A

##### *Materials*

1,5-Cyclooctadiene (cod), trifluoromethanesulfonic acid, thiophene-2-carbonitrile and *N,N*-dimethylformamide (DMF) were purchased from Aldrich-Sigma Chemical Inc. and dried with CaH<sub>2</sub> before use. All reagents, unless otherwise stated, were obtained from Sigma Aldrich and were used without further purification.

## **Section B** *Instruments*

$^1\text{H}$  NMR spectra were recorded using a Bruker AV-400 spectrometer in  $\text{CDCl}_3$  as a solution, with tetramethylsilane (TMS) as the internal reference, and chemical shifts were recorded in ppm. Solid state  $^{13}\text{C}$  NMR spectrum was obtained on a Bruker AV-500 spectrometer operating at 75.5MHz. Infrared measurements were performed on a Thermo Nicolet Nexus 470 Fourier transform infrared spectroscopy (FT-IR), and spectra were recorded from in the range of  $4000\text{-}400\text{ cm}^{-1}$  using the KBr pellet technique on a FTIR spectrum GX instrument. Thermogravimetric analysis (TGA) was performed on a Mettler TGA thermogravimetric analysis instrument in the nitrogen atmosphere at a heating rate of  $10^\circ\text{C}/\text{min}$  from 50 to  $800^\circ\text{C}$ . Scanning electron microscopy (SEM) and Energy-dispersive X-ray spectroscopy (EDS) experiments were performed on a FEI Quanta-200 scanning electron microscope. Transmission electron microscopes (TEM) were performed on a JEM-2100F transmission electron microscope. Powder X-ray diffraction (PXRD) was obtained on a BD-86 X-ray diffractometer. The XPS measurements were carried out with a K-Alpha 1063 spectrometer using a monochromated  $\text{Al-K}_\alpha$  ( $1486.5\text{ eV}$ ) X-ray radiation. Glass transition temperatures ( $T_g$ ) were determined with a Mettler DSC822 DSC instrument in flowing nitrogen at a heating rate of  $10\text{ }^\circ\text{C min}^{-1}$  from 100 to  $400\text{ }^\circ\text{C}$ .

Polymer surface areas and pore size distributions were measured by

nitrogen adsorption and desorption at 77 K using the ASAP 2020 volumetric adsorption analyzer. The apparent surface areas ( $S_{\text{BET}}$ ) for  $\text{N}_2$  were calculated using the Brunauer-Emmett-Teller (BET) model in the relative pressure ( $P/P_0$ ) range from 0.04 to 0.32. Porous volume was calculated using the BJH method. The adsorption/desorption isotherms of  $\text{CO}_2$  on CMP-CSU13 were obtained from the ASAP2020 volumetric adsorption analyzer at 273 K and 298 K up to 1bar. Samples were degassed at 200 °C for 10 h under vacuum ( $10^{-5}$  bar) before analysis.

## Section C Experimental Sections

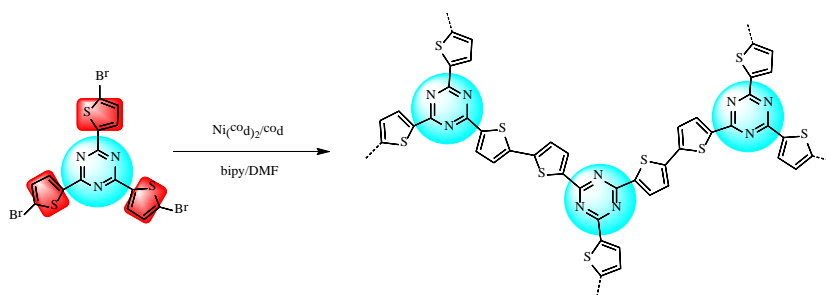
### *Synthesis of 2,4,6-tri(thiophen-2-yl)-1,3,5-triazine*

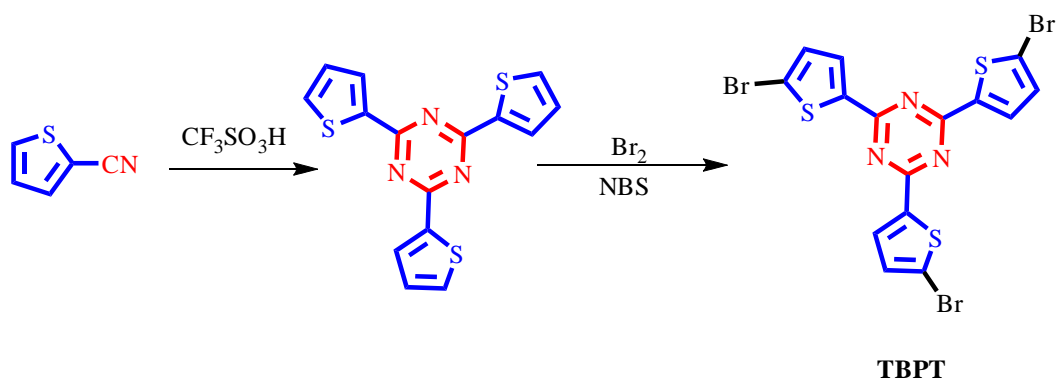
To a vigorously stirred solution of trifluoromethanesulfonic acid (30.0 g, 0.2 mol) was dropwisely added thiophene-2-carbonitrile (10.9 g, 0.1 mol) in dry  $\text{CHCl}_3$  (100 mL) over the course of 1 h at 0 °C under  $\text{N}_2$ . After stirring for a further 1 h at 0 °C, the mixture was stirred another for 24h at ambient temperature and was poured into water containing a few drops of  $\text{NH}_4\text{OH}$ . Then the resultant mixture was filtered, and the residue was collected and purified by column chromatography using petroleum as an eluent to afford a white solid (9.82 g, Yield: 90%). M.p: 192-193 °C; MALDI-TOF/MS ( $\text{M}^+$  Calcd. as  $\text{C}_{15}\text{H}_9\text{N}_3\text{S}_3$ , 326.9959) m/z: 326.5874 ( $\text{M}^+$ );  $^1\text{H}$  NMR ( $\text{CDCl}_3$ , 400 MHz):  $\delta$  7.97 (m, 3 H), 7.63 (m, 3 H), 7.21 (m, 3 H); FTIR (KBr,  $\text{cm}^{-1}$ ): 1598, 1511, 1412, 1380.

### *Synthesis of 2,4,6-Tris(5-bromothiophen-2-yl)-1,3,5-triazine (TBTP)*

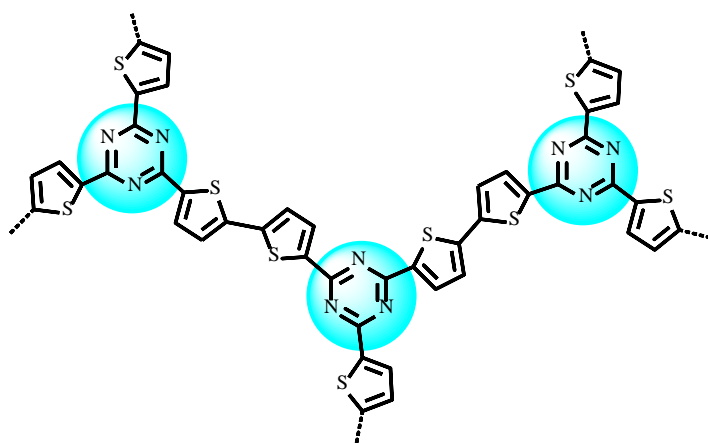
The synthesis route to starting monomer TBPT and its intermediate are outlined in Scheme S1. The intermediate 2,4,6-tri(thiophen-2-yl)-1,3,5-triazine was almost quantitatively prepared in a revised procedure 30. For the efficient synthesis of the halogenide building block, two strategies of bromination employing liquid bromine and N-bromobutanamide were combined, reducing content of byproducts

such as monobromo-substituted derivatives and dibromo substituted derivatives, thereby greatly increasing the yield of the target compound. To a solution of 2,4,6-tri(thiophen-2-yl)-1,3,5-triazine (0.98 g, 3 mmol) in  $\text{CHCl}_3$  (20 mL) was added an excess amount of *N*-bromosuccinimide (2.14 g, 12 mmol) in portions. The reaction was stirred at room temperature for 3 d, then liquid bromine (1.59 g, 10 mmol) was dropwisely added into the mixture. After stirring for another 2 day, the mixture was washed with saturated  $\text{NaHSO}_3$  and  $\text{NaHCO}_3$ , the organic phase was dried with anhydrous  $\text{Na}_2\text{SO}_4$  and concentrated under vacuum. The crude product was recrystallized with ethanol to afford a pale yellow solid. Yield: 95%. M.p: 253-254 °C; MALDI-TOF/MS ( $M^+$  Calcd. as  $\text{C}_{15}\text{H}_6\text{Br}_3\text{N}_3\text{S}_3$ , 562.7254)  $m/z$ : 562.2326 ( $M^+$ );  $^1\text{H}$  NMR ( $\text{CDCl}_3$ , 400 MHz):  $\delta$ 7.97 (d, 3 H), 7.18 (d, 3 H); FTIR (KBr,  $\text{cm}^{-1}$ ): 1601, 1521, 1417,1352, 480.





**Scheme S1** Synthetic route to CSU-CMP 13 and the starting monomer TBPT



### *Synthesis of CMP-CSU13 spheres*

1,5-Cyclooctadiene (cod, 7.30 mmol, dried over  $\text{CaH}_2$ ) was added to a solution of bis(1,5-cyclooctadiene)nickel(0) ( $[\text{Ni}(\text{cod})_2]$ , 7.30 mmol) and 2,2'-bipyridyl (1.14 g, 7.30 mmol) in dry dimethylformamide (DMF) (120 mL), and the mixture was stirred until completely dissolved. 2,4,6-Tris(5-bromothiophen-2-yl)-1,3,5-triazine (1.05 g, 1.86 mmol) in dry dimethylformamide (DMF) (120 mL) was subsequently added to the resulting purple solution. The reaction vessel was heated at  $100\text{ }^\circ\text{C}$  for 24 h, then heat up to  $110\text{ }^\circ\text{C}$  for 48 h under a nitrogen atmosphere. After cooling to room temperature, concentrated HCl was added to obtain a deep purple suspension. After filtration, the residue was washed by  $\text{CHCl}_3$ ,

tetrahydrofuran (THF) and H<sub>2</sub>O, respectively, and dried in vacuo to give CMP-CSU13 as brown powders. Yield: 83%.

*General procedure for the formation of CMP-CSU13 nanotubes*

1,5-Cyclooctadiene (cod, 7.30 mmol, dried over CaH<sub>2</sub>) was added to a solution of bis(1,5-cyclooctadiene)nickel(0) ([Ni(cod)<sub>2</sub>], 7.30 mmol) and 2,2'-bipyridyl in dry dimethylformamide (DMF) (120 mL). Notably, twice-times amount of 2,2'-bipyridyl (2.28 g, 14.60 mmol) and a few drops of 1,2-dibromoethane (0.3 mL, 7.3 mmol) were charged, and then the mixture was stirred until completely dissolved and heating to 70 °C for 2h. 2,4,6-Tris(5-bromothiophen-2-yl)-1,3,5-triazine (1.05 g, 1.86 mmol) in dry dimethylformamide (DMF) (150 mL) was subsequently added to the resulting purple solution. The reaction vessel was heated at 100 °C for 24 h, then heat up to 110 °C for 48 h under a nitrogen atmosphere. After cooling to room temperature, concentrated HCl was added to the deep purple suspension, after filtration, the residue was washed by CHCl<sub>3</sub>, tetrahydrofuran (THF) and H<sub>2</sub>O, respectively, and dried in vacuo to give a brown powder. Yield: 71%.

50 mg of the obtained powder and 10 mL ethanol were added to a centrifuge tube, the mixture was firstly sonicated for 5 minutes at room temperature, then filtered and dried under infrared. The obtained tubular like CMP-CSU13 was characterized using SEM and TEM.

**Section D** Mechanism of Yamamoto-Ullmann coupling reaction

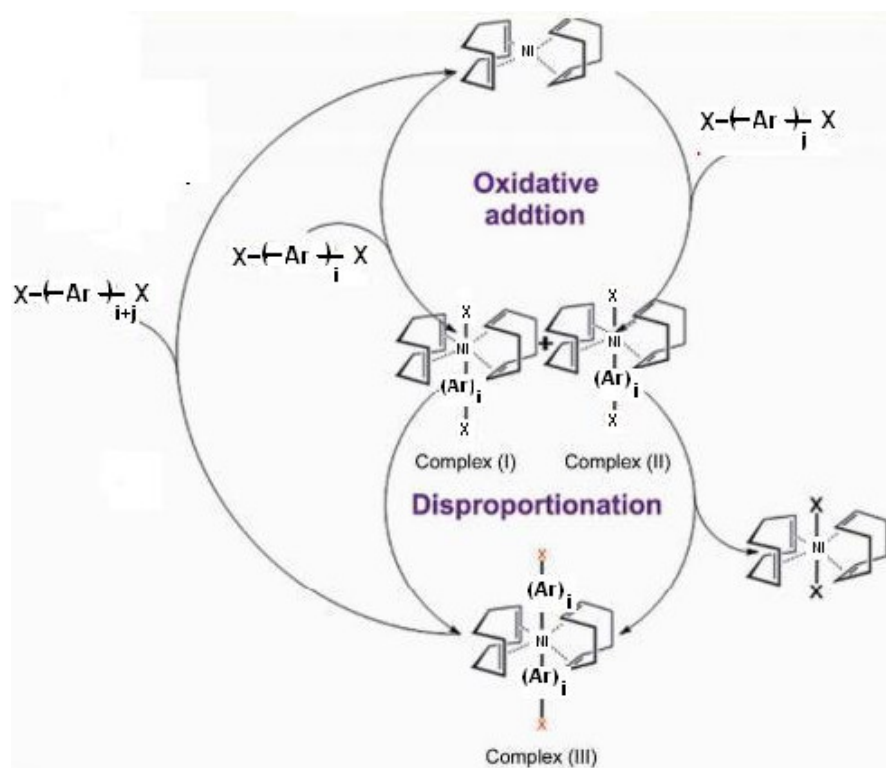


**Fig. S1** Mechanism of Yamamoto-Ullmann coupling reaction<sup>S1</sup>

## Section E Transmission Electron Microscopy of nanocrystals

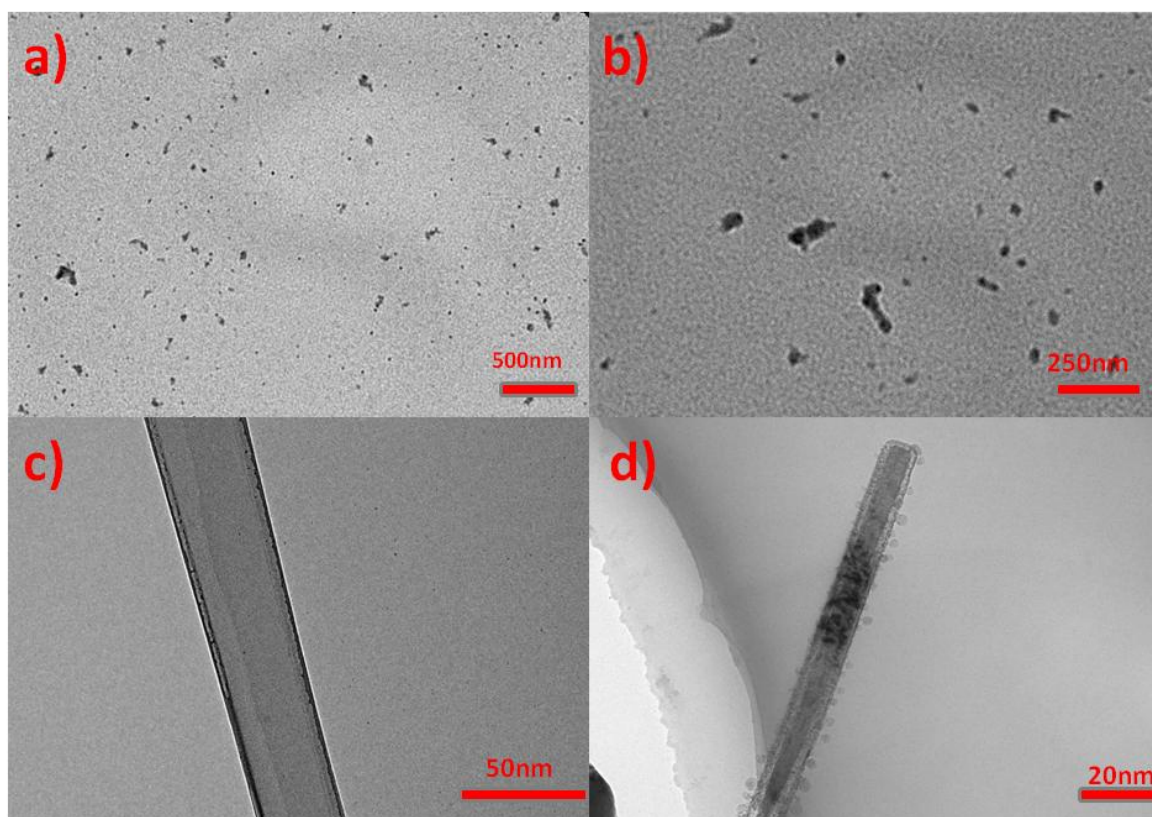


**Fig. S2** TEM images of nanocrystals(a: 500 nm; b: 250 nm; c: 50 nm; d: 20 nm)

**Section F Spectral characterization of monomers and CSU-CMP networks**

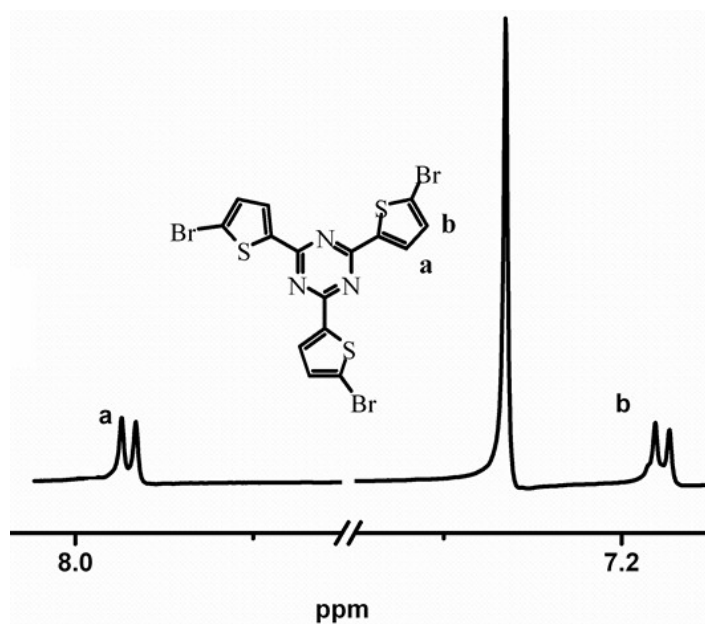


**Fig. S3** <sup>1</sup>H NMR spectrum of monomer TBPT

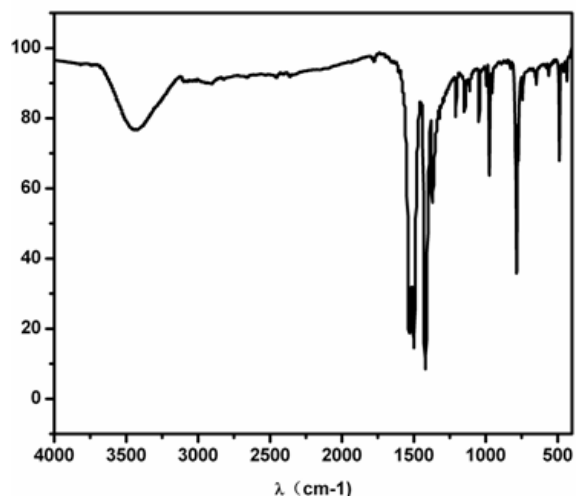


**Fig. S4** FT-IR spectrum of monomer TBPT

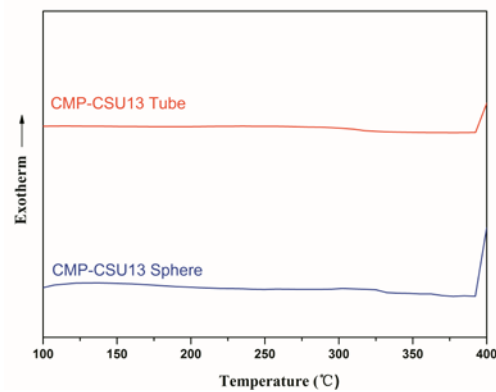


**Fig. S5** DSC traces of tubular CMP-CSU13 (red) and sphere-like CMP-CSU13(blue) under nitrogen

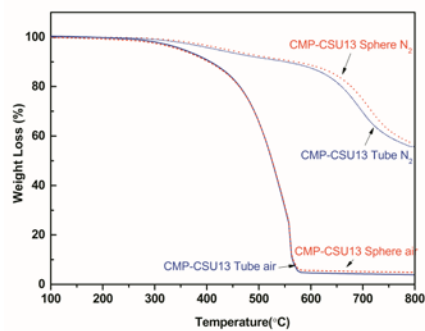


**Fig. S6** TGA traces of tubular CMP-CSU13 (blue) and sphere-like CMP-CSU13(red) under nitrogen and air atmosphere

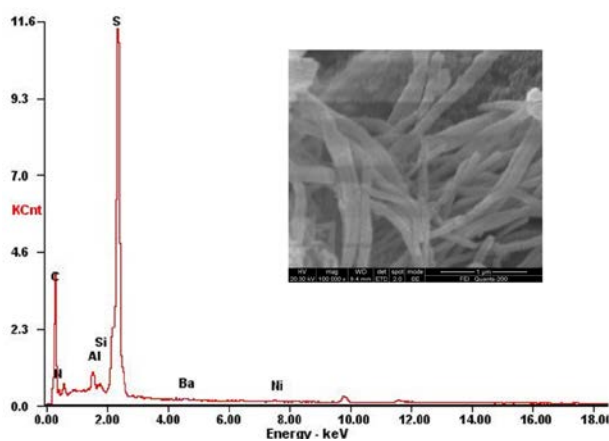


**Fig. S7** SEM EDS mapping of CMP-CSU13 tubes

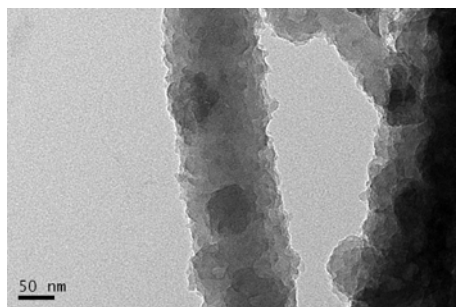
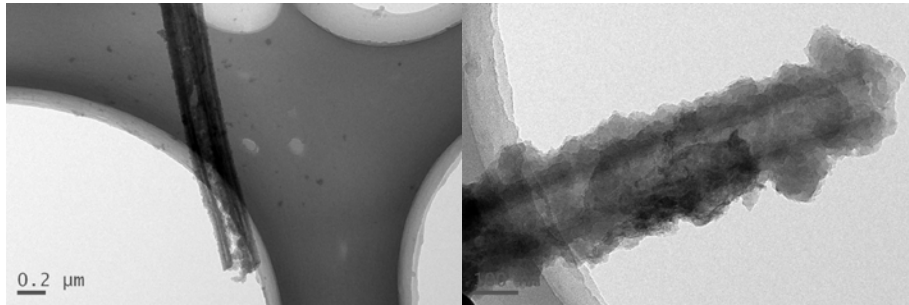
## Section G Elemental analysis

**Table S1** Elemental analysis data of the polymers

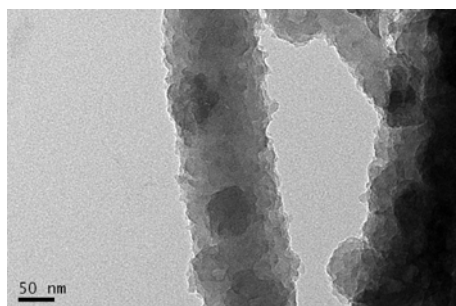
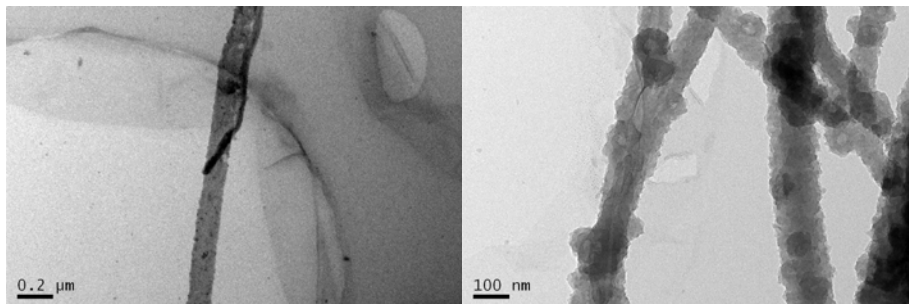
Sample	Found(%)				Calculated(%)			
	C	H	N	S	C	H	N	S
CMP-CSU13Tube	55.53	1.86	12.95	29.65	54.49	1.79	13.16	29.86
CMP-CSU13Sphere	55.53	1.86	12.95	29.65	54.82	1.77	13.03	29.27

## Section H Morphology study

a)  $150 \pm 10$  nm



b)  $120 \pm 10$  nm



c)  $90 \pm 10$  nm

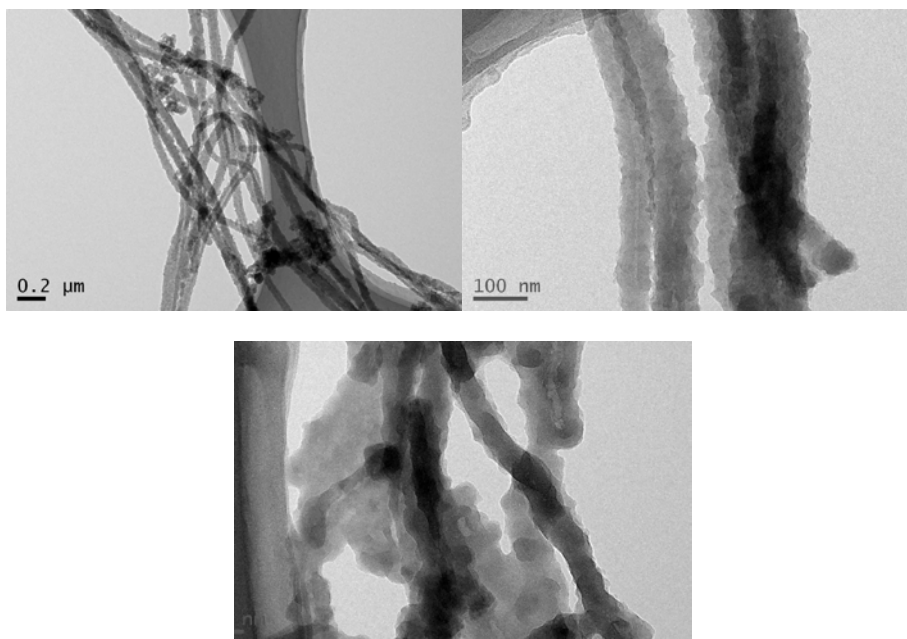


**Fig. S8** TEM images of CMP-CSU13 tubes generated under different polymerization conditions

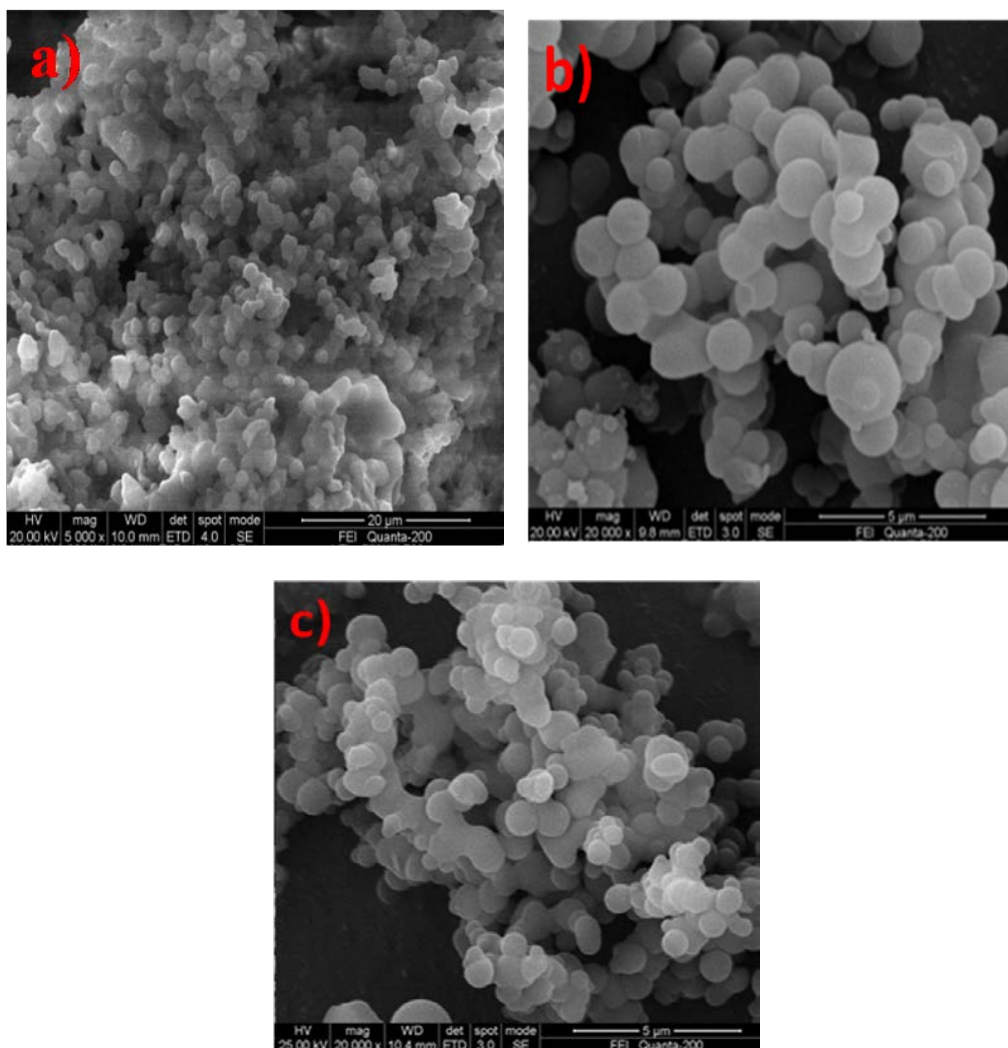


**Fig. S9** SEM images of CMP-CSU13 spheres generated under different polymerization conditions (Entry 0: a, b; Entry 1: c)

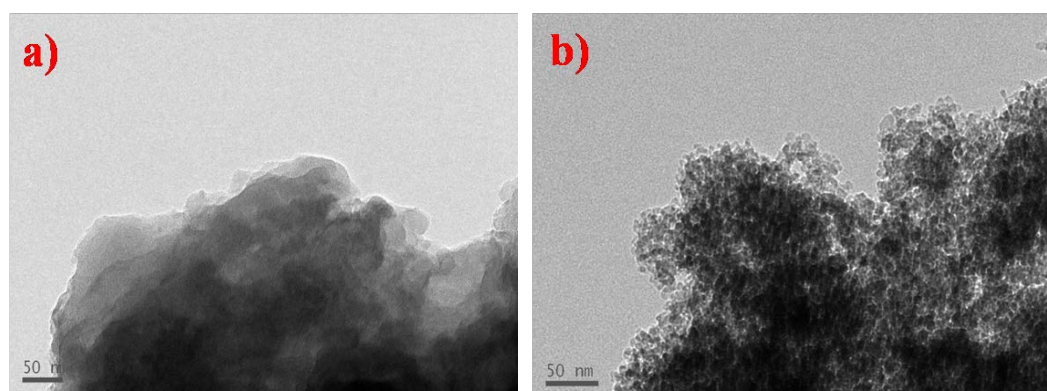


**Fig. S10** TEM images of CMP-CSU13 spheres generated under different polymerization conditions

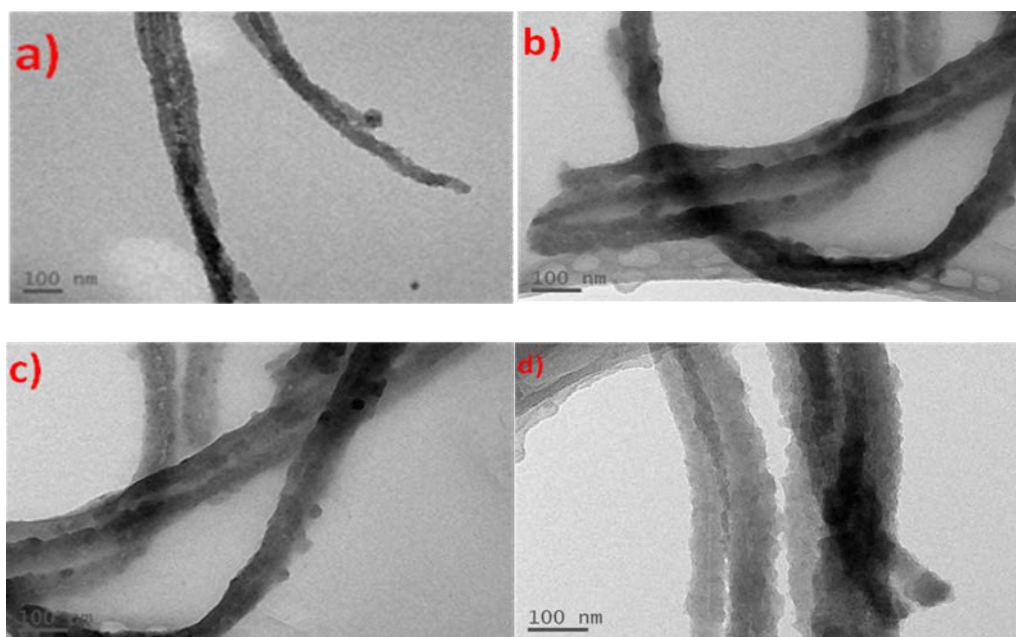


**Fig. S11** TEM images of CMP-CSU13 tube after dispersion in different solvents (a: ethanol; b: *n*-hexane; c: water; d: acetone)

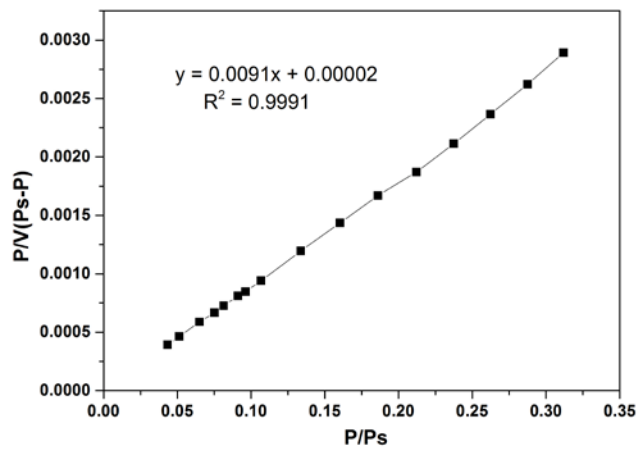


**Fig. S12** Multiple point BET plot of CMP-CSU13 tube

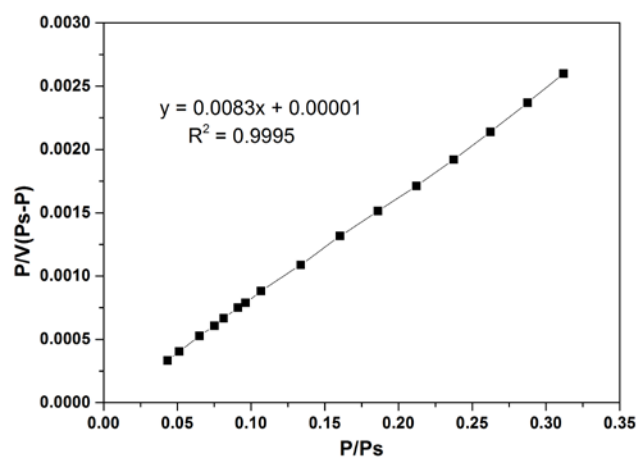


**Fig. S13** Multiple point BET plot of CMP-CSU13 sphere

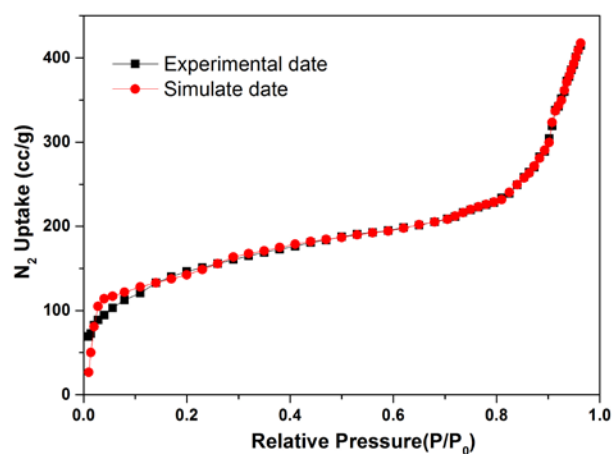


**Fig. S14** NL-DFT fit between the simulated data (red circle) and the experimental data ( $N_2$  physisorption, measured at 77 K; black square) for CMP-CSU13 tube

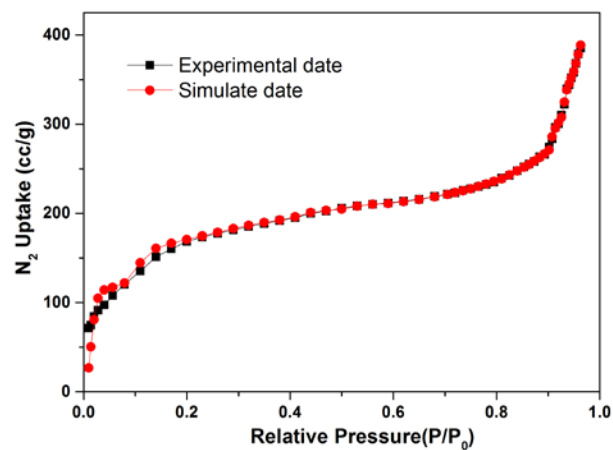


**Fig. S15** NL-DFT fit between the simulated data (red circle) and the experimental data ( $N_2$  physisorption, measured at 77 K; black square) for CMP-CSU13 sphere

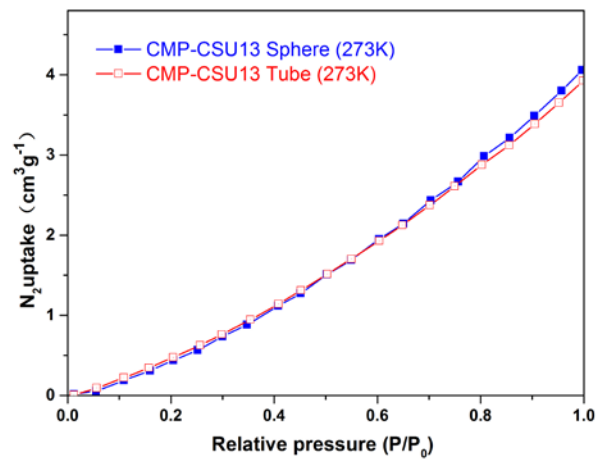


**Fig. S16**  $N_2$  adsorption isotherms of CMP-CSU13 at 273 K

## Section I Polymerization conditions and porous properties

**Table S2** Polymerization conditions and parameters of CMP-CSU13 tubes

Entry	Polymerization conditions			Nanotubes		
	2,2'-bipyridyl (mmol)	1,2-dibromoethane (mmol)	TBPT/DMF (mmol/mL)	Length (nm)	Diameter (nm)	Note
0	7.3	0	1.86/120	-	180±20	Sphere Fig. S9a,b,S10a
1	7.3	0	1.86/240	-	120±20	Sphere Fig. S9c,S10b
2	14.6	7.3	1.86/120	2-4	120±10nm	Fig.2c, Fig. S7b
3	18.2	10.9	1.86/120	2-4	150±10nm	Fig. S7a
4	10.8	3.6	1.86/120	2-4	90±10nm	Fig. S7c
5	14.6	7.3	1.86/240	2-4	90±10nm	Fig. S7c

**Table S3** The properties of porosity, gas uptake of CMP-CSU13

Sample	$S_{\text{BET}}$ ( $\text{m}^2/\text{g}$ )	$V_{\text{Micro}}^{\text{a}}$ ( $\text{cc g}^{-1}$ )	$V_{\text{total}}^{\text{b}}$ ( $\text{cm}^3 \text{g}^{-1}$ )	Size <sup>c</sup> (nm)	$\text{CO}_2^{\text{d}}$ (wt%)
CMP-CSU13Tube	741	0.99	0.43	0.76	13.6
CMP-CSU13 Sphere	763	1.07	0.49	0.71	14.3

<sup>a</sup> Micropore volume determined from the  $\text{N}_2$  isotherm at  $P/P_0=0.1$ ; <sup>b</sup> Total pore volume determined from the  $\text{N}_2$  isotherm at  $P/P_0=0.99$ ;  
<sup>c</sup> Dominant pore size; <sup>d</sup>  $\text{CO}_2$  uptake at 273K/1bar.

## Section J Isothermic heat of adsorption

The isosteric heat of adsorption,  $Q_{st}$ , defined as

$$Q_{st} = RT^2 \left( \frac{\partial \ln p}{\partial T} \right)_q \quad (1)$$

was determined using the pure component isotherm fits using the Clausius-Clapeyron equation.<sup>s2</sup>

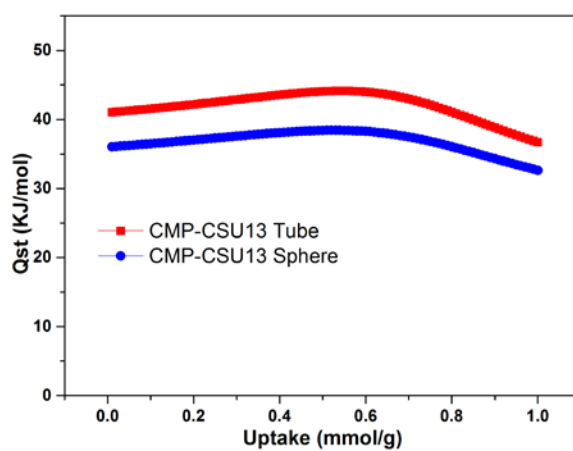


**Fig. S17** Plots of isosteric heat of adsorption ( $Q_{st}$ ) for CO<sub>2</sub> of CMP-CSU13 versus CO<sub>2</sub> uptake

## Section K IAST Selectivity

The selectivity of preferential adsorption of component 1 over component 2 in a mixture containing 1 and 2, perhaps in the presence of other components too, can be formally defined as

$$S_{ads} = \frac{q_1/q_2}{P_1/P_2} \quad (2)$$

In equation (2),  $q_1$  and  $q_2$  are the absolute component loadings of the adsorbed phase in the mixture. These component loadings are also termed the uptake capacities. In all the calculations to be presented below, the calculations of  $q_1$  and  $q_2$  are based on the use of the Ideal Adsorbed Solution Theory (IAST) of Myers and Prausnitz.<sup>S3</sup> The accuracy of the IAST calculations for estimation of the component loadings for several binary mixtures in a wide variety of zeolites, and MOFs has been established by comparison with Configurational-Bias Monte Carlo (CBMC) simulations of mixture adsorption.<sup>s2-4</sup>

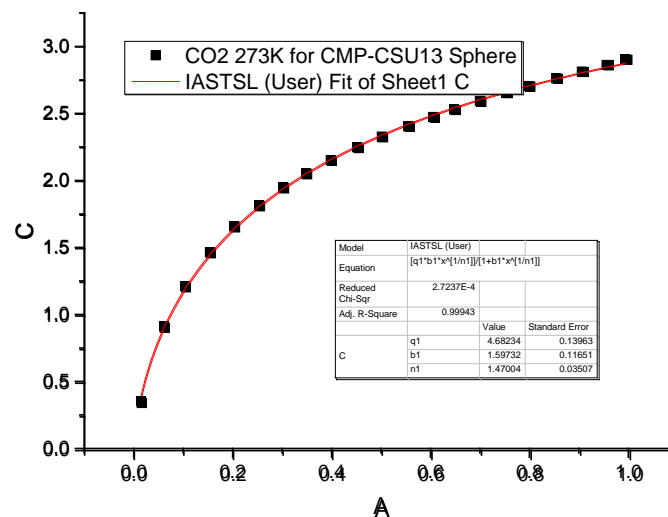


**Fig.S18** CO<sub>2</sub> isotherm of CMP-CSU13 sphere fitted by single-site Langmuir equation

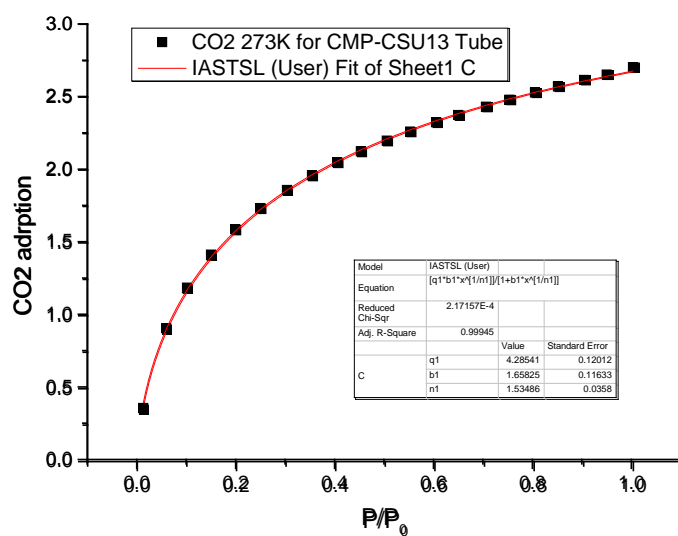


**Fig.S19** CO<sub>2</sub> isotherm of CMP-CSU13 tube fitted by single-site Langmuir equation

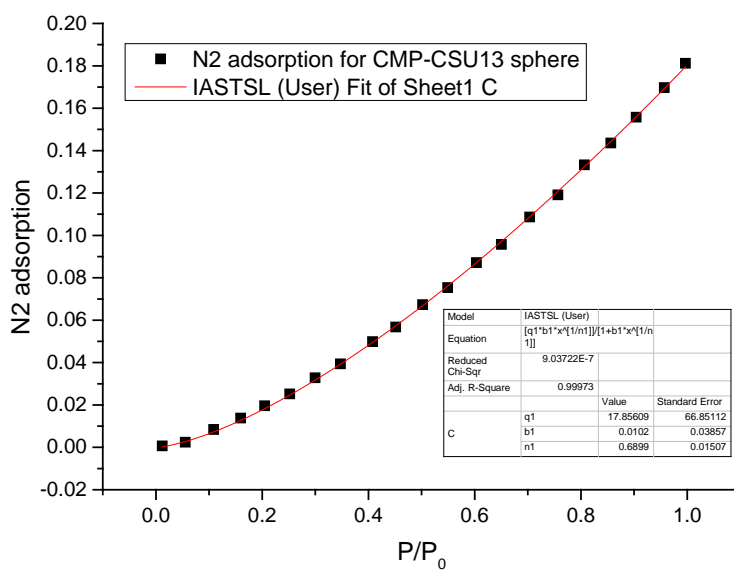


**Fig.S20** N<sub>2</sub> isotherm of CMP-CSU13 sphere fitted by single-site Langmuir equation

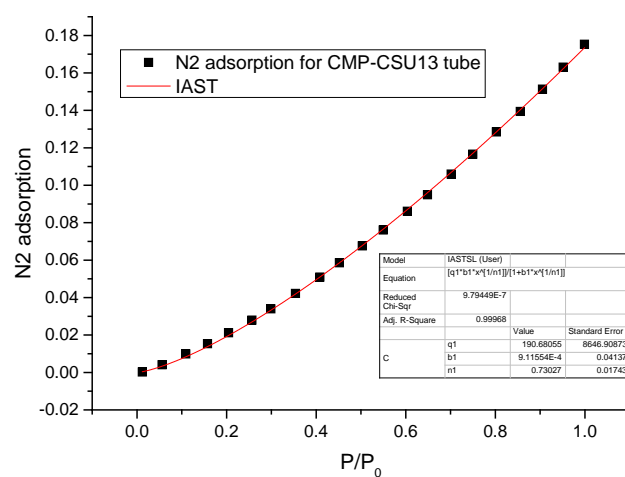


**Fig.S21** N<sub>2</sub> isotherm of CMP-CSU13 tube fitted by single-site Langmuir equation

## References

- S1 Ben, T., & Qiu, S. CrystEngComm, 2013, 15(1), 17-26.  
 S2 H. Wu, K. Yao, Y. Zhu, B. Li, Z. Shi, R. Krishna, J. Li, J. Phys. Chem. C 2012, 116, 16609.  
 S3. A. L. Myers, J. M. Prausnitz, A.I.Ch.E.J. 1965, 11, 121.  
 S4. R. Krishna, J. M. van Baten, Chem. Eng. J. 2007, 133, 121.